Journal of Materials and Electronic Devices 1(2015) 44-49



Synthesis and physical characterization of $LiXO_2$ (X=Ni, Mn, Co, Cu) Nanocomposites for Li Ion Batteries

M. Sasmaz
Department of Physics, Faculty of Science, Fırat University, Elazığ, Turkey

In present study, we prepared $LiXO_2$ (X=Ni, Mn, Co, Cu) nanocomposites with various chemical routes and studied chemical structural and morphological properties depends on transition metal. XRD patterns indicated that the LiXO2 nanocomposites are polycrystalline. The chemical compositions of the composites and vibrations were confirmed by Energy disperse X-Ray (EDX) and Fourier transform infrared spectroscopy (FTIR) results. Scanning electron microscopy (SEM) images were carried out to investigate the microstructure nanocomposites. SEM results indicate that the nanocomposites are formed from the nanoparticles and the size of nanocomposites were changed depend on transition metal.

Keywords: Li ion batteries, Nanocomposites, XRD, FTIR, SEM

Submission date:01 June 2015
Acceptance date:19. August 2015

Corresponding authors: merivansasmaz@gmail.com

1. Introduction

Li ion batteries (LIB) attract a lot attention for using in portable electronic devices and hybrid electric vehicles. Nowadays, the development of electrode materials for LIB has become quite necessary to require the existence of a higher power electrical appliances, high capacity, long life and good rate. Nanosize electrode materials are promising candidates for LIB which have many advantages. These advantages are as follows: i) Li ion transitions are damaging in the micro-size metal oxide structure but which perform reversible reactions without harming in the nanosize. ii) electron transport increase with small grain size which provide high Li ion flux. iii) the chemical potential of Li ion and electrons shows improvement with the smaller particle size [1-4].

Lithium oxide nanocomposites are used as source of Li ion for safety considerations. Lithium cobalt oxide show high density but suffer from high cost and chemical instability. Compared to lithium nickel oxide with lithium cobalt oxide, which has higher specific capacity but it is also electrochemically and thermally less resolute [5]. $LiMnO_2$ and $LiCuO_2$ nanocomposites are known nontoxic and low cost material as a cathode electrode for LIB [6-10].

In present work, $LiXO_2$ (X= Ni, Mn, Co, Cu) nanocomposites were successfully synthesized with various chemical routes. The aim of the study is to compare the structural, chemical and morphological properties of nanocomposites between each other and reported studies..

2. Experimental details

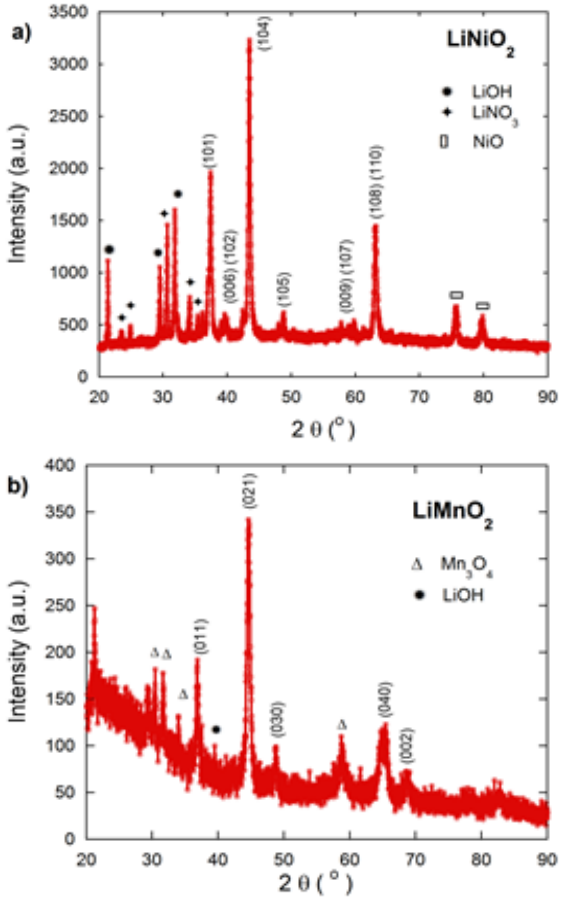
Firstly, the weights of selected materials (lithum nitrate, nikel acetate, mangane nitrate, cobalt nitrate and copper nitrate) calculated by using equal n (Li nitrate)/ n(X) = 4 mmol. In a typical synthesis, 1 mmol nikel acetate was dissolved in 30 ml distilled water with ultrasonic blender and 4 mmol lithum nitrate was added to solution then continued ultrasonication. After solving, ammonia solution (25%) was added to the solution until pH value reached to around neutral. The obtained solution was kept on a magnetic stirrer for 2 hours and was placed in the oven at 90 oC heat treatment for 24 hours. The remained material was washed and again exposed to heat treatment placed in the oven at 120 oC for 5 hours. Finally, the LiNiO2 nanocomposite annealed in the ash furnace at 500 oC for 5 hours. The rest nanocomposites were prepared with the same route of $LiNiO_2$ nanocomposite.

The composition of nanocomposites were determined by using an energy disperse X-Ray (EDX) with belong to SEM. The structral properties were investigated by using a Rigaku X-ray diffractometer (XRD). Fourier

transform infrared spectrometer (FTIR) with an ID5 ATR sample holder was used for chemical bonding. The morphological characterization were carried out by using a SM -7001F mark scanning electron microscope (SEM).

3. Results and discussion

Figure 1 show XRD patterns of LİXO$_2$ (X=Ni, Mn, Co, Cu) nanocomposites. Figure 1.a exhibited that LiNiO2 nanocomposite has many crystalline peaks of $LiNiO_2$ and a few peaks of unreacted lithium compounds such as LiOH, $LiNO_3$ and NiO. The main peak of $LiNiO_2$ has a rhombohedral structure with a space group R-3m. Figure 1. b shows $LiMnO_2$ XRD pattern, which indexed as orthorhombic phase with a space group of Pmmn. $LiMnO_2$ nanocomposite has many orthorhombic peaks of $LiMnO_2$ and a few peaks of the mixture of manganese acetate aqueous solution such as Mn_3O_4 and LiOH aqueous solution. Figure 1 c shows XRD pattern of $LiCoO_2$ nanocomposite, which can be indexed with a space group R-3m. The peaks are corresponding to crystalline structures of $LiCoO_2$ and also pattern exhibits a few peaks of LiOH aqueous solution similar to Fig1 a-b. Figure 1 d shows XRD pattern of $LiCuO_2$ nanocomposite. The peaks are corresponding to crystalline structures of $LiCuO_2$ and also pattern exhibits a few peaks of LiOH aqueous solution similar to Fig1 a-c The obtained structural properties of all nanocomposites agree with reported results [10-15].



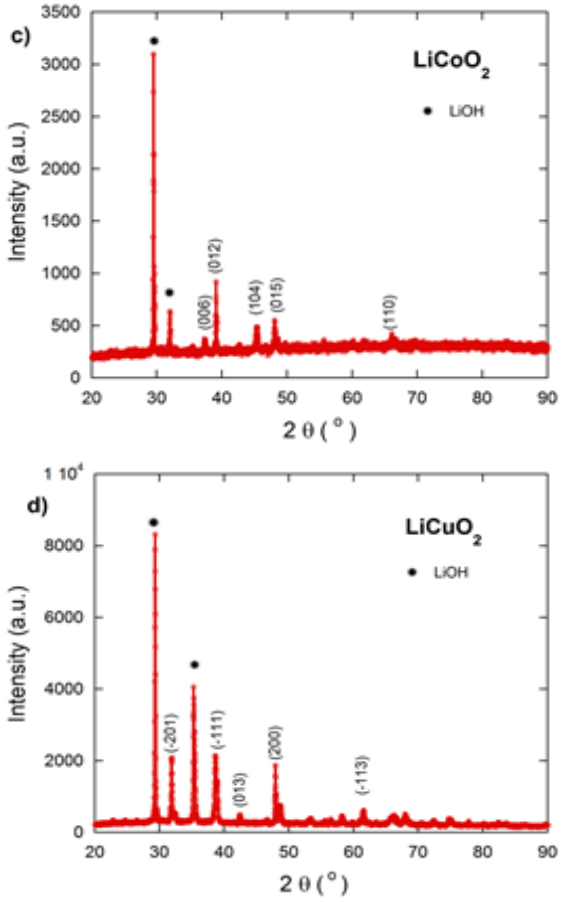


Figure 1- XRD patterns of all nanocomposites a) $LiNiO_2$, b) $LiMnO_2$, c)$LiCoO_2$ and d) $LiCuO_2$.

The crystallite size of all nanostructures are calculated using the Debye–Scherrer equation and given in Table 1.

$$D = \frac{0.9\lambda}{\beta \cos\theta}$$

In equation, λ is wavelengh of XRD (Cu Kα), β (FWHM) is the full width at half-maximum of the main peak and θ is the Bragg diffraction angle. The crystallite sizes of all nanocomposites are different than each other and $LiCoO_2$ nanocomposite has the maximum value. The FWHM depend on the length and stacking defects of the crystals. $LiMnO_2$ nanocomposite has the largest FWHM value which is higher than the results of reported by H. Ji et al [16].

Table 1. XRD parameters of all nanocomposites

Nanocomposite	h	k	l	2 θ (°)	FWHM	D (nm)
$LiNiO_2$	1	0	4	43.48	0.480	8.909
$LiMnO_2$	0	2	1	45.04	0.805	5.342

$LiCoO_2$	0	1	2	39.12	0.284	14.843
$LiCuO_2$	-1	1	1	38.68	0.525	8.018

The compositions of the $LiXO_2$ (X= Ni, Mn, Co, Cu) nanocomposites were determined by EDX shown in Figure 2a-d. Expected elements were observed from EDX spectrums. There are some impurity peaks, which represent gold because of coating with gold during measurement. The atomic percentage of Ni was 12 % in $LiNiO_2$, the atomic percentage of Mn was 22 % in $LiMnO_2$, the atomic percentage of Co was 26 % in $LiCoO_2$, the atomic percentage of Cu was 15% in $LiCuO_2$ nanocomposite.

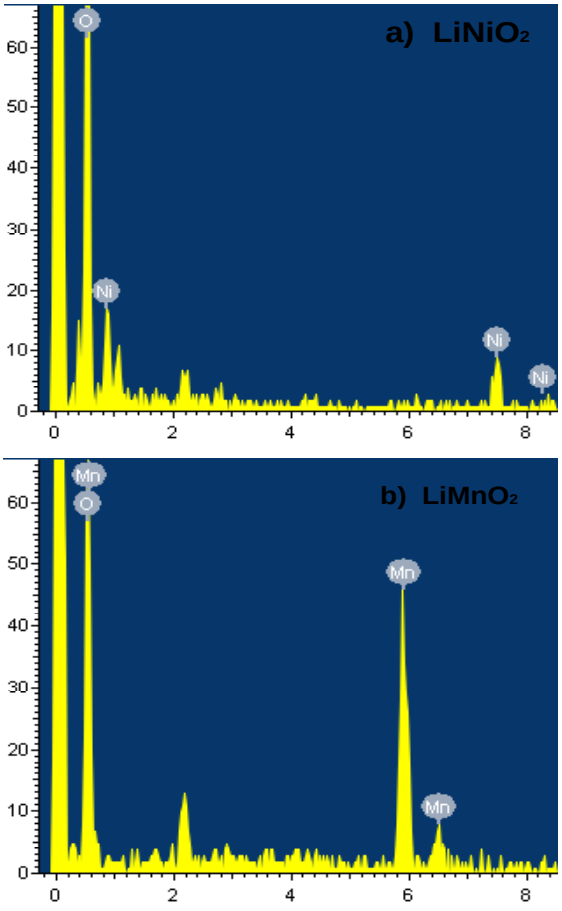


Figure 2- EDX analysis of all nanocomposites a) $LiNiO_2$, b) $LiMnO_2$, c)$LiCoO_2$ and d) $LiCuO_2$

Fourier transform infrared spectroscopy (FTIR) measurements of nanocomposites are shown in Figure 3. For $LiNiO_2$ composite (see Fig.3-a), a wide the O-H stretching band is observed around 3100-3700 cm-1 which infers that there is no nickel hydroxide and lithium hydroxide [17]. The bands were observed at 1640 and 1345 cm-1 can be assigned to C-O-O and bands of carboxyl group seen at 595, 738, 860 and 1085 cm-1 corresponding to metal citrate [18]. The vibrations of $LiMnO_2$ has four peaks at 1424, 1085, 860 and 627 cm-1 which are corresponding to C-C, C-H, C-H and Mn-O respectively (Fig 3b) [19]. For $LiCoO_2$ nanocomposite (see Fig 3c), the broad band around of 3400 cm-1 can be attribute to oxidation state of Co and to random distribution of Li+ ions and hydroxyl group [20]. The peak of 2430 cm-1 is corresponding to O-H band. The small peaks of 1790 and 1640 cm-1 and the sharp characteristic peaks of around 1330 cm-1 are attributed to carbonyl group (COO) with metal ions [20]. The band of C-H and O-Co-Co vibrations are observed at 1050 and 590 cm-1, respectively [21]. The vibration characteristic of $LiCuO_2$ nanocomposite is similar to $LiCoO_2$ nanocomposite with different peak at 590 cm-1, which is corresponding to O-Cu-Cu (Fig 3d). Also the broad band around of 3400 cm-1 can be attribute to oxidation state of Cu and to random distribution of Li+ ions and hydroxyl group.

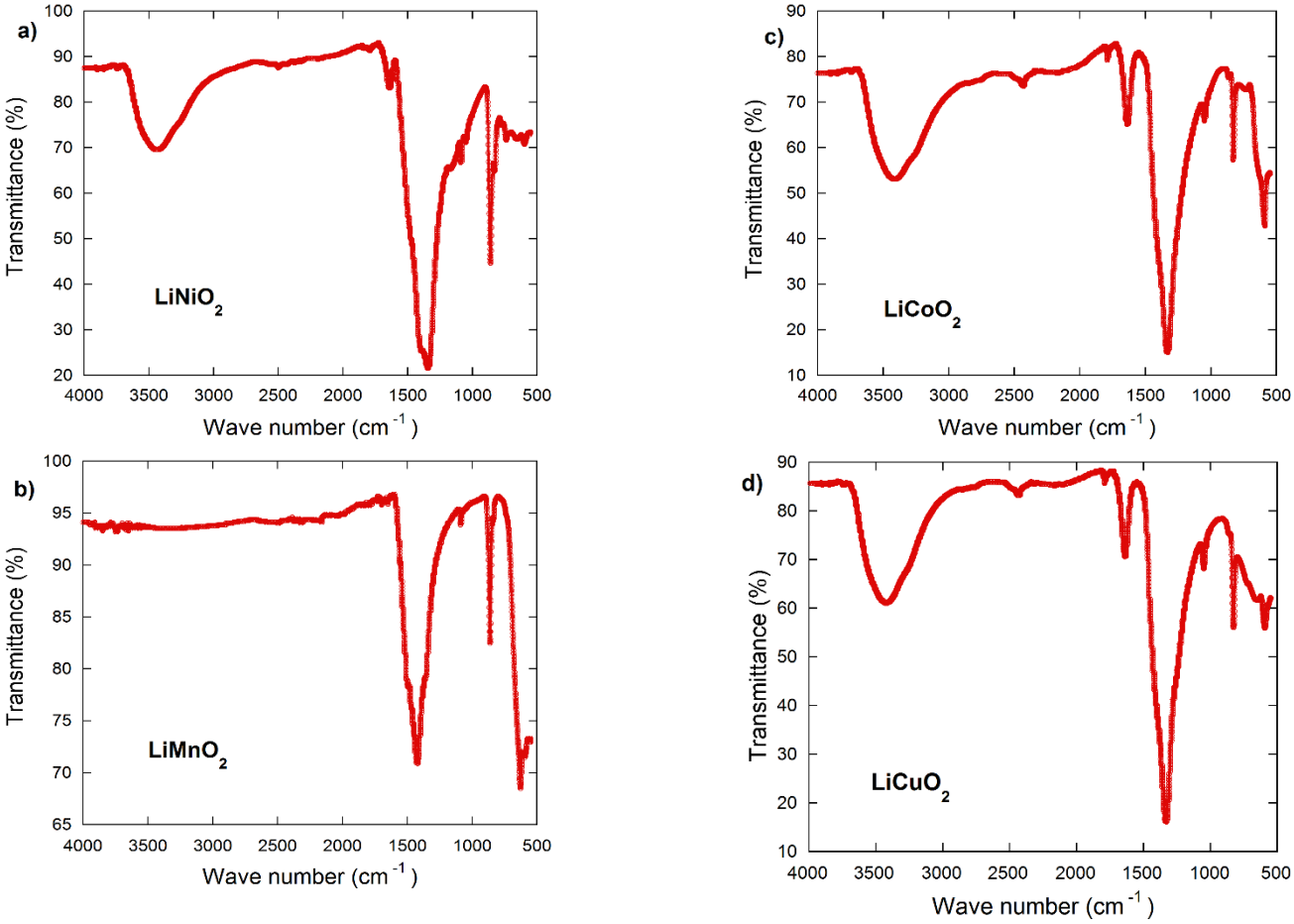


Figure 3. FTIR analysies of all nanocomposites

Scanning electron micrographs are shown in Figure 4. Micrographs of all nanocomposites were done with 100 nm size and 50000 X magnification for image quality. $LiNiO_2$ nanocomposite exhibits spherical structure with 35-85 nm the average diameters and homogeneous distribution of nanoparticles (Fig. 4a). It can be seen that nanoparticles are very fine and the size are smaller than the SEM results reported by Chang et al [17]. $LiMnO_2$ composite has complex morphology as spherical like cauliflower structure with 60-276 nm the average diameters and shows similar size with the results reported by H.Ji et al (Fig. 4b) [16]. Also the size of $LiMnO_2$ is larger than $LiNiO_2$ nanocomposite. $LiCoO_2$ composite has fine distribution and diagonal shape with 80-290 nm the average diameters(Fig. 4c), which indicates similar size with report of Yang et al [21]. $LiCuO_2$ nanocomposite has diagonal shape with 330-830 nm the average diameters and is generally larger than the rest composites (Fig. 4d). The morphology of nanocomposites is changed depending on the transition metal.

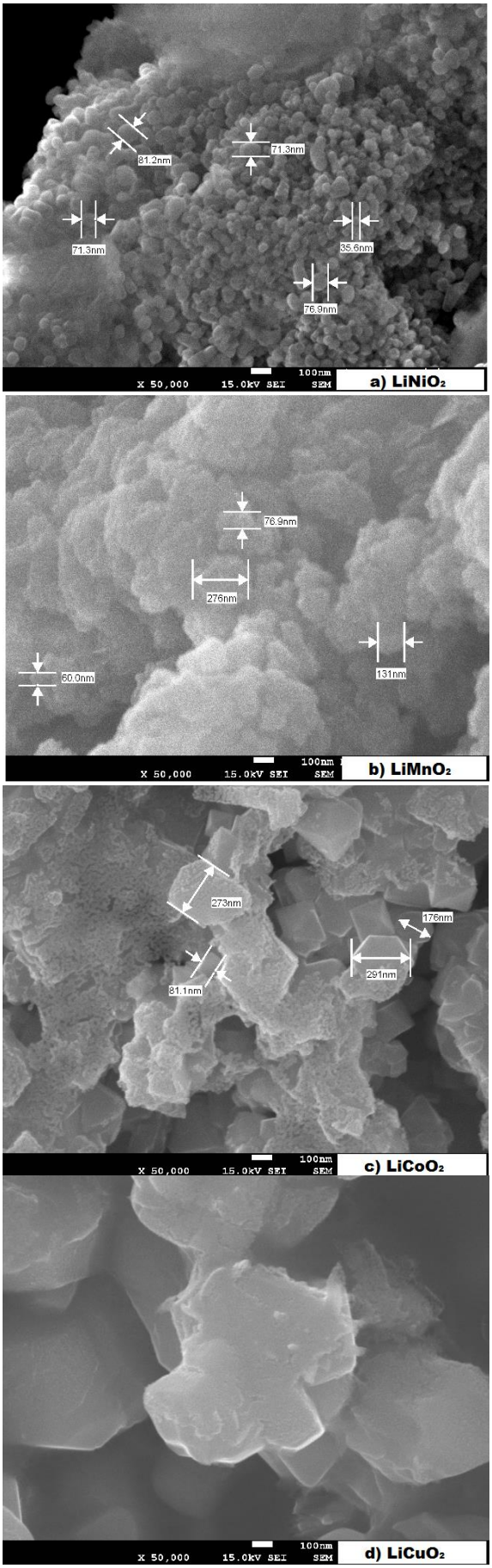


Figure 4. SEM micrographics of all nanocomposites

Conclusions

$LiXO_2$ (X= Ni, Mn, Co, Cu) nanocomposites were synthesized successfully through various chemical routes. The results of EDX confirm all elements which must be present in all nanocomposites. XRD results show crystalline structure of nanocomposites. The crystallite sizes of all nanocomposites are different and $LiCoO_2$ nanocomposite has the maximum value. The chemical characterization results (FTIR) indicate the bands which should be exist in vibrations. SEM micrographs demonstrate that the morphology of nanocomposites is changed depending on the transition metal and the average diameters align as $LiNiO_2$ < $LiMnO_2$ < $LiCoO_2$ < $LiCuO_2$ nanocomposite.

References:

[1] P. Kalyani, N. Kalaiselvi (2005) Various aspects of $LiNiO_2$ chemistry: A review, Science and Technology of Advanced Materials 6: 689–703.
[2] M.K. Song, S. Park, F. M. Alamgir, J. Cho, M. Liu (2011) Nanostructured electrodes for lithium-ion and lithium-air batteries: the latest developments, challenges, and perspectives, Materials Science and Engineering R 72: 203–252.
[3] N. Alias, A.A. Mohamad (2015) Advances of aqueous rechargeable lithium-ion battery: A review, Journal of Power Sources 274: 237-251.
[4] B. Scrosati, J. Garche (2010) Lithium batteries: Status, prospects and future, Journal of Power Sources 195: 2419–2430.
[5] A.W. Moses, H. G. G. Flores, J.G. Kim, M. A. Langell (2007) Surface properties of $LiCoO_2$, $LiNiO_2$ and $LiNi_{1_x}Co_xO_2$, Applied Surface Science 253: 4782–4791.
[6] G., Wang, S., Zhou, H., Wang, Z., Ren, J., Bai (2015) Preparation of Carbon-Coating Layer by Ethyne Thermal Decomposition and Its Effects on the Improvement of Lithium Storage Properties for Co_3O_4 Hexagonal Micro-Platelets, Science of Advanced Materials 7: 1272-1281.
[7] Z. Li, L. Wang, X. Ge, H. Ge, and L. Yin (2014) Nickel Oxide Nanoparticles/Ordered Mesoporous Carbon Nanocomposites as Anode Materials, for Lithium-Ion Battery with Improved Electrochemical Performance, Science of Advanced Materials 6: 2089-2097.
[8] Y.R., Tao, W.W., Xiong, X.C., Wu (2014) Titanium Tri- and di-Sulfide Nanobelts/Graphene Composites for Rechargeable Lithium Battery Cathodes and Enhancement of Reversible Capacities, Science of Advanced Materials 6: 1965-1972.
[9] H. Arai, S. Okada, Y. Sakurai, J. Yamaki (1998) Electrochemical and structural study of Li CuO , LiCuO and $NaCuO_2$, Solid State Ionics 106: 45–53.
[10] S.T. Myung, S. Komaba, N. Kumagai (2002) Hydrothermal synthesis and electrochemical behavior of orthorhombic $LiMnO_2$, Electrochimica Acta 47: 3287-3295.
[11] Y.M. Choi, S.I. Pyun, S.I. Moon , Y.E. Hyung (1998) A study of the electrochemical lithium intercalation behavior

of porous LiNiO electrodes prepared by solid-state reaction and sol–gel methods, Journal of Power Sources 72: 83–90.
[12] M.Y.Song, R. Lee (2002) Synthesis by sol–gel method and electrochemical properties of $LiNiO_2$ cathode material for lithium secondary battery, Journal of Power Sources 111: 97–103.
[13] C.H. Lu, H.C. Wang (2004) Reverse-microemulsion preparation and characterization of ultrafine orthorhombic $LiMnO_2$ powders for lithium-ion secondary batteries, Journal of the European Ceramic Society 24: 717–723.
[14] Y. Ou, J. Wena, H. Xu, S. Xie, J. Li (2013) Ultrafine $LiCoO_2$ powders derived from electrospun nanofibers for Li-ion batteries, Journal of Physics and Chemistry of Solids 74: 322–327.
[15] Y. Arachi, T. Setsu, T. Ide, K. Hinoshita, Y. Nakata (2012) Reversible electrochemical reaction of CuO with Li in the $LiCuO_2$ system, Solid State Ionics 225: 611–614.
[16] H. Ji, G. Yang, X. Miao, A. Hong (2010) Efficient microwave hydrothermal synthesis of nanocrystalline orthorhombic $LiMnO_2$ cathodes for lithium batteries, Electrochimica Acta 55: 3392–3397.
[17] C.C., Chang, P.N. Kumta (1998) Particulate sol–gel synthesis and electrochemical characterization of $LiMO_2$ (M= Ni, Ni0.75Co0.25) powders, Journal of Power Sources 75: 44–55.
[18] S.P. Lin, K.Z. Fung, Y.M. Hon, M.H. Hon (2001), Crystallization mechanism of $LiNiO_2$ synthesized by Pechini method, Journal of Crystal Growth 226: 148–157.
[19] C. Liu, J. Nan, X. Zuo, X. Xiao, D. Shu (2012) Synthesis and Electrochemical Characteristics of an Orthorhombic $LiMnO_2$ Cathode Material Modified With Poly (Vinyl-Pyrrolidone) for Lithium Ion Batteries, International Journal of Electrochemical Science 7: 7152 – 7164.
[20] W.D. Yang, C.Y. Hsieh, H.J. Chuang, Y.S. Chen (2010) Preparation and characterization of nanometric-sized $LiCoO_2$ cathode materials for lithium batteries by a novel sol–gel method, Ceramics International 36: 135–140.
[21] J. Cao, G. Hu, Z. Peng, K. Du, Y. Cao (2015) Polypyrrole-coated $LiCoO_2$ nanocomposite with enhanced electrochemical properties at high voltage for lithium-ion batteries, Journal of Power Sources 281: 49-55..